Total Transfer Capability of Meshed Transmission Grids with VSC-HVDC Considering Control Parameter Uncertainties: Concept and Calculation

Yanbo Chen, Tong Han, Zeli Wang
Sch. of Electrical and Electronic Engineering
North China Electric Power University
Beijing, China 102206
Email: yanbochen2008@sina.com

Shujun Wang
Mudanjiang Power
Industry School
Mudanjiang, China, 157011
Email: 2236200569@qq.com

Jin Ma
Sch. of Electrical and Information Engineering
University of Sydney
NSW, 2006, Australia
Email: majinjm@gmail.com

***Abstract*—This paper addresses the issue of control parameter uncertainties in total transfer capability (TTC) calculation for meshed transmission grids with VSC-HVDC. A new concept of TTC embodying control parameter uncertainties (TTCU) is first proposed. And then the calculation model of TTCU for meshed transmission grids with VSC-HVDC and its solving approach are further presented. Simulations are carried on the modified IEEE 39-bus system, illustrating that control parameter uncertainties can decrease TTC and impact the optimal operation of VSC-HVDC with respect to TTC, and the proposed TTCU providing robust operation mode for VSC-HVDC is superior to TTC.**

***Index Terms*—Total transfer capability, control parameter uncertainties, VSC-HVDC, optimization.**

I. Introduction

Today the technology of voltage source converter based high voltage direct current transmission (VSC-HVDC) has been widely applied in power grids. Owing to superior control characters, VSC-HVDC has more merits compared with traditional transmission technologies. A key benefit of VSC-HVDC is that it can significantly improve the transfer capability of interconnected transmission grids. And thus the research on transfer capability of meshed transmission grids with VSC-HVDC is essential to the cost-benefit assessment of VSC-HVDC and operation of the meshed girds [1]–[3].

Some measures including total transfer capability (TTC), available transfer capability and transmission reliable margin, are vital in the issue of transfer capability. And among them, TTC calculation is the fundamental component. By definition, TTC represents the amount of the electric power that can be transferred over interconnected transmission networks in a reliable manner while meeting a specified set of defined per- and post-contingency system conditions [4].

Although various approaches have been developed for the calculation of TTC of AC grids, there are fewer proposed for the meshed transmission grids with VSC-HVDC. In [5] and [6], an available transfer capability calculation approach based on the optimal power flow (OPF) model for meshed VSC-HVDC transmission grids is proposed. However, the calculation model in [5] and [6] omits N-1 security constraints, and control modes of VSCs and corresponding control parameters are fixed in the OPF model. And thus this approach is unable to embody the effect of control characters of VSCs on transfer capability of meshed transmission grids with VSC-HVDC. And [7] gives a TTC calculation approach for meshed VSC-HVDC transmission grids that accurately models the $N-1$ security constraints and post-$N-1$ contingency VSC-HVDC control constraints, by extending the OPF model to multiple operation states. Compared with the approach in [5] and [6], that in [7] is competent to show the improvement of TTC due to the superior control characters of VSC-HVDC, compute TTC and furnish optimal control modes of VSCs and corresponding optimal values of control parameters simultaneously.

Due to various kinds of uncertainties in control systems, e.g., the noise in electrical devices and errors in control system inputs, control parameters of VSCs can be realized only to a certain degree of accuracy. And control parameter uncertainties naturally cause the following questions: 1) What effects do control parameter uncertainties have on TTC and how to embody this effect in TTC calculation? 2) Do the optimal control modes of VSCs and corresponding optimal values of control parameters remain unchanged when considering the control parameter uncertainties? Furthermore, these two questions are vital to the cost-benefit assessment of VSC-HVDC and the optimal operation of the meshed girds, respectively.

To address the issue of control parameter uncertainties of VSCs in TTC calculation, this paper firstly proposes a concept of TTC considering control parameter uncertainties, called TTCU for short. And then based on our previous work in [7], the TTCU calculation model for meshed transmission grids with VSC-HVDC and its solving approach are presented. Finally, using the modified IEEE 39-bus system, effects of control parameter uncertainties on TTC and the optimal operation of VSC-HVDC, and the merits of TTCU are demonstrated.

II. Background of VSC-HVDC

A. Steady-state Model of VSC-HVDC

Fig. 1 illustrates VSC-HVDC connected with the AC grid. Assuming converters to be with the modular multilevel converter technology, filters are omitted in this paper. And

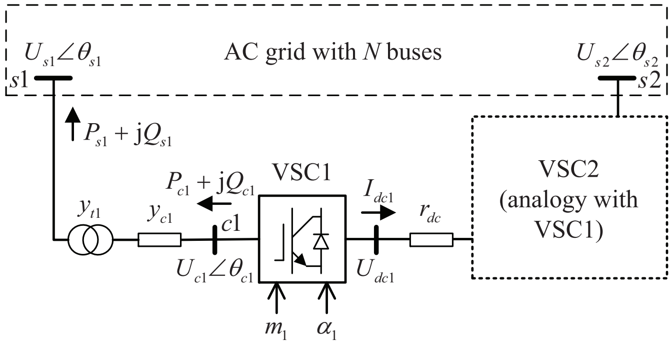

Fig. 1. Illustration of VSC-HVDC connected to the AC grid.

taking the VSC1 as an example, it is connected with AC system through a phase reactor with a complex admittance $y_{c1}=g_{c1}+jb_{c1}$ and a converter transformer represented by its admittance $y_{t1}=g_{t1}+jb_{t1}$. The equations for the power flowing to the AC grid from the converter transformer can thus be written as

$$P_{s1}=-U_{s1}^2g_{tc1}+U_{s1}U_{c1}\left(g_{tc1}\cos\alpha_1+b_{tc1}\sin\alpha_1\right) \quad (1)$$

$$Q_{s1}=U_{s1}^2b_{tc1}+U_{s1}U_{c1}\left(g_{tc1}\sin\alpha_1-b_{tc1}\cos\alpha_1\right) \quad (2)$$

where $U_{s1}\angle\theta_{s1}$ and $U_{c1}\angle\theta_{c1}$ represent the complex voltage of bus $s1$ and bus $c1$, respectively. $\alpha_1=\theta_{s1}-\theta_{c1}$ is called phase-shifting angle. And g_{tc1} and b_{tc1} are the real part and the image part of the equivalent complex admittance $y_{tc1}=y_{t1}+y_{c1}$, respectively. The equations of the power flow at converter side can be written as

$$P_{c1}=U_{c1}^2g_{tc1}-U_{c1}U_{s1}\left(g_{tc1}\cos\alpha_1-b_{tc1}\sin\alpha_1\right) \quad (3)$$

$$Q_{c1}=-U_{c1}^2b_{tc1}+U_{c1}U_{s1}\left(g_{tc1}\sin\alpha_1+b_{tc1}\cos\alpha_1\right) \quad (4)$$

The equation for the active power balance of converters is expressed as

$$P_{dc1}+P_{loss1}+P_{c1}=0 \quad (5)$$

with P_{dc1}, the DC power of VSC1, given by

$$P_{dc1}=U_{dc1}I_{dc1} \quad (6)$$

where U_{dc1} and I_{cd1} denote the DC voltage and the DC current of VSC1, respectively.

And P_{loss1} in (5), denoting the active power loss of VSC1, is given by

$$P_{loss1}=a_1+b_1I_{ac1}+c_1I_{ac1}^2 \quad (7)$$

where a_1, b_1 and c_1 are the loss coefficients of VSC1. It is noted that the value of c_1 varies with the operation state of VSC1. And I_{ac1}, denoting the current magnitude, is expressed as

$$I_{ac1}=\sqrt{\left(g_{tc1}+b_{tc1}\right)\left(U_{c1}^2+U_{s1}^2-2U_{c1}U_{s1}\cos\alpha_1\right)}. \quad (8)$$

Besides, U_{c1} and U_{dc1} satisfy the following equation:

$$U_{c1}=\frac{M_1U_{dc1}}{\sqrt{2}} \quad (9)$$

where M_1 is the modulation index. And (9) constitutes a coupling between the AC and DC converter sides.

For the DC grid, the following equations are satisfied:

$$I_{dc1}=\frac{U_{dc1}-U_{dc2}}{r_{dc}}. \quad (10)$$

B. Control of VSC-HVDC

A VSC can independently control the active and reactive power injection w.r.t the AC grid. Taking the VSC1 in Fig. 1 as an example, the active power injection control can be realised in two different ways: constant P_{s1} and constant U_{dc1}. And the reactive power injection control can also be realised in two ways: constant Q_{s1} and constant U_{s1}. Thus control modes of the VSC1 includes: (1) constant P_{s1} and Q_{s1}, (2) constant P_{s1} and U_{s1}, (3) constant U_{dc1} and Q_{s1}, and (4) constant U_{dc1} and U_{s1}. And the control mode of the VSC2 is analogy. In this paper, four common forms of combinations of control modes of converters are considered for a two-terminal VSC-HVDC: (3)+(1), (3)+(2), (1)+(4) and (2)+(4), called combination 1 to 4 for short respectively.

Considering that the control parameters of VSCs can be realized only to a certain degree of accuracy, we model its uncertainties as independent truncated normal distributions [8]. For example, given a fixed value P'_{s1} for the constant P_{s1} control, the probability density function of $\delta_{P_{s1}}=P_{s1}-P'_{s1}$ is given by

$$f(\delta_{P_{s1}})=\begin{cases}\dfrac{\frac{1}{\sigma}\phi\left(\frac{\delta_{P_{s1}}-\mu}{\sigma}\right)}{\Phi\left(\frac{\bar{t}-\mu}{\sigma}\right)-\Phi\left(\frac{\underline{t}-\mu}{\sigma}\right)} & \underline{t}\le\delta_{P_{s1}}\le\bar{t}\\ 0 & \text{otherwise}\end{cases}. \quad (11)$$

Here μ, σ, $\underline{t}$ and $\bar{t}$ denote mean, standard deviation, lower tail and upper tail of the distribution, respectively. And $\phi(\cdot)$ is the probability density function of the standard normal distribution and $\Phi(\cdot)$ is its cumulative distribution function. The truncated normal distributions as given in (11) is denoted by $\Pi(\mu,\sigma,\underline{t},\bar{t}$ in the following parts of this paper.

III. TTCU and its Calculation for Meshed Transmission Grids with VSC-HVDC

A. The Concept of TTCU

The basic idea of TTCU is to regard TTC as a random variable causing by the parameter uncertainties and compute the expected value of TTC. Let C and C_u represent TTC and TTCU of power grids respectively, then TTCU is defined as

$$C_u=\mathrm{E}\left[C\right]=\int_\Omega C\mathrm{d}P \quad (12)$$

with (Ω,P) representing the probability space of the random variable C.

Further, denoting the vector of parameter uncertainties as $\boldsymbol{\delta}$, (12) can be rewritten as

$$C_u=\int C\left(\boldsymbol{\delta}\right)p\left(\boldsymbol{\delta}\right)\mathrm{d}\boldsymbol{\delta} \quad (13)$$

where $p\left(\boldsymbol{\delta}\right)$ is the joint density of parameter uncertainties. And $C\left(\boldsymbol{\delta}\right)$ represents the functions of TTC w.r.t. $\boldsymbol{\delta}$.

B. Calculation Model for TTCU of Meshed Transmission Grids with VSC-HVDC

Based on (13) and the TTC calculation model proposed in [7], the TTCU calculation model for meshed transmission grids with VSC-HVDC is mathematically modeled as the following optimization problem:

$$C_u = \max \quad \left\{ \int F\left(\boldsymbol{x}^s, \boldsymbol{u}_1^s, \boldsymbol{u}_2^s + \boldsymbol{\delta}_{u_2}, \boldsymbol{\phi}\right) p\left(\boldsymbol{\delta}_{u_2}\right) \mathrm{d}\boldsymbol{\delta}_{u_2} \right\} \tag{14a}$$

$$s.t. \quad \boldsymbol{h}^s(\boldsymbol{x}^s, \boldsymbol{u}_1^s, \boldsymbol{u}_2^s + \boldsymbol{\delta}_{u_2}, \boldsymbol{\phi}) = \boldsymbol{0} \;\; s \in \Xi \tag{14b}$$

$$\underline{\boldsymbol{g}}^s \leq \boldsymbol{g}^s(\boldsymbol{x}^s, \boldsymbol{u}_1^s, \boldsymbol{u}_2^s + \boldsymbol{\delta}_{u_2}, \boldsymbol{\phi}) \geq \overline{\boldsymbol{g}}^s \;\; s \in \Xi \tag{14c}$$

$$\boldsymbol{l}\left(\boldsymbol{x}^s, \boldsymbol{u}_1^s, \boldsymbol{u}_2^s + \boldsymbol{\delta}_{u_2}, \boldsymbol{\phi}\right) = \boldsymbol{0} \tag{14d}$$

where $F(\cdot)$ is the computing function of transfer capability. Ξ is the set of operation states of power grids, including the normal operation state and operation states after a $N-1$ contingency. And $\boldsymbol{x}^s$ and $\boldsymbol{u}_1^s$ denote the vectors of state variables of the optimization model and variable regulating variables of power grids both in the operation state s, respectively. $\boldsymbol{u}_2^s$ and $\boldsymbol{\delta}_{u_2}$ denote the vectors of control parameters of VSCs in the operation state s and its uncertainties, respectively. $\boldsymbol{\phi}$ is the vector of auxiliary variables. And $\underline{\boldsymbol{g}}^s$ and $\overline{\boldsymbol{g}}^s$ represent lower and upper bounds of inequality constraints for the operation state s. (14b) and (14c) denote equality constraints and inequality constraints for various operation states respectively. And (14d) expresses equality constraints coupling different operation states.

In the following part, we first provide the nomenclature, and detailed expressions of the model are then given from aspects of the objective function, and the three kinds of constraints.

1) Nomenclature:

s_1	The normal operation state of power grids.
$s_i (i \neq 1)$	Operation states after a $N-1$ contingency.
N	The set of buses in power grids.
N_A	The set of buses disconnected with VSCs.
n_D	The total number of VSC-HVDC systems.
A_i, B_i	The rectifier side and inverter side connecting buses of the ith VSC-HVDC system.
N_D	$N_D = \{A_1, B_1, A_2, B_2, \cdots, A_{n_d}, B_{n_d}\}$
$N_D{}'$	$N_D{}' = \{(A_1, B_1), \cdots, (A_{n_d}, B_{n_d})\}$
N_G	The set of generators in power grids.
N_L	The set of load buses in power grids.
L	The set of AC branches in power grids.
$y_{ij}^{s_k}$, $g_{ij}^{s_k}$, $b_{ij}^{s_k}$	The entry of nodal admittance matrix in state s_k relating to bus i and bus j, its real and imaginary part.
S_O	The set of buses in the source area.
S_I	The set of buses in the sink area.
L_A, L_D	The set of AC tie lines and DC tie lines.
$U_i^{s_k} \angle \theta_i^{s_k}$	Complex voltage of bus i in operation state s_k.
$U_{c,i}^{s_k} \angle \theta_{c,i}^{s_k}$	Complex voltage of AC side of the converter connected to bus $i \in N_D$ in operation state s_k.
$U_{dc,i}^{s_k}, I_{dc,i}^{s_k}$	Voltage of DC side of the converter connected to bus $i \in N_D$ and current from this side, both in operation state s_k.
δ_υ	Uncertainties of υ with υ denoting a parameter of $\boldsymbol{u}_2^s$.
$P_{L,i}^{s_k}$, $Q_{L,i}^{s_k}$	Active and reactive load power of bus i in operation state s_k.
$P_{G,i}^{s_k}$, $Q_{G,i}^{s_k}$	Active and reactive generator power of bus i in operation state s_k.
$P_{S,i}^{s_k}$, $Q_{S,i}^{s_k}$	Active and reactive power injected into bus i from the connected VSC in operation state s_k
$g_{tc,i}, b_{tc,i}$	Real part and image part of the equivalent complex admittance of the VSC connected with bus i.
$r_{dc,ij}$	Resistance of the DC line between $(i,j) \in N_D{}'$.

2) Objective function: With TTC expressed as the form of transmission power through tie lines between the source and the sink area, the function $F(\cdot)$ is give by

$$F = \sum_{l \in L_A \cup L_D} P_l^{s_1} \tag{15}$$

with $P_l^{s_1}$ denoting transmission active power in the sending terminal of the line l in the normal operation state. The expression of $P_l^{s_1}$ is given as

$$P_l^{s_1} = \begin{cases} {U_i^{s_1}}^2 g_{ij}^{s_1} - U_i^{s_1} U_j^{s_1} \left(g_{ij}^{s_1} \cos\theta_{ij}^{s_1} + b_{ij}^{s_1} \sin\theta_{ij}^{s_1}\right) & l \in L_A \\ \left(U_{dc,i}^{s_1} + \delta_{U_{dc,i}}\right) \dfrac{U_{dc,i}^{s_1} + \delta_{U_{dc,i}} - U_{dc,j}^{s_1} - \delta_{U_{dc,j}}}{r_{dc,ij}} & l \in L_D \end{cases} \tag{16}$$

$$F' = \int \left[\sum_{l \in L_A} {U_i^{s_1}}^2 g_{ij}^{s_1} - U_i^{s_1} U_j^{s_1} \left(g_{ij}^{s_1} \cos\theta_{ij}^{s_1} + b_{ij}^{s_1} \sin\theta_{ij}^{s_1}\right) + \sum_{l \in L_D} \left(U_{dc,i}^{s_1} + \delta_{U_{dc,i}}\right) \frac{U_{dc,i}^{s_1} + \delta_{U_{dc,i}} - U_{dc,j}^{s_1} - \delta_{U_{dc,j}}}{r_{dc,ij}} \right] p\left(\boldsymbol{\delta}_{u_2}\right) \mathrm{d}\boldsymbol{\delta}_{u_2} \tag{18}$$

$$\begin{aligned} &{U_{c,i}^{s_k}}^2 g_{tc,i} - U_{c,i}^{s_k} \left(U_{s,i}^{s_k} + \delta_{U_{s,i}}\right) \left(g_{tc,i} \cos\alpha_i^{s_k} - b_{tc,i} \sin\alpha_i^{s_k}\right) + \left(U_{dc,i}^{s_k} + \delta_{U_{dc,i}}\right) \frac{U_{dc,i}^{s_k} + \delta_{U_{dc,i}} - U_{dc,j}^{s_k} - \delta_{U_{dc,j}}}{r_{dc,ij}} + a_i + c_i (g_{tc,i} + b_{tc,i}) \\ &\times \left({U_{c,i}^{s_k}}^2 + \left(U_{s,i}^{s_k} + \delta_{U_{s,i}}\right)^2 - 2U_{c,i}^{s_k} \left(U_{s,i}^{s_k} + \delta_{U_{s,i}}\right) \cos\alpha_i^{s_k}\right) + b_i \sqrt{(g_{tc,i} + b_{tc,i}) \left({U_{c,i}^{s_k}}^2 + \left(U_{s,i}^{s_k} + \delta_{U_{s,i}}\right)^2 - 2U_{c,i}^{s_k} \left(U_{s,i}^{s_k} + \delta_{U_{s,i}}\right) \cos\alpha_i^{s_k}\right)} = 0 \end{aligned} \tag{21}$$

where i and j denote the sending and receiving terminal buses of tie line l for $l \in L_A$ respectively. And $(i,j) \in N_D{}'$ and is connected by tie line l for $l \in L_D$. And thus the objective function in (14a) denoted as F' for short can be written as (18).

3) Constraints $\boldsymbol{h}^s\left(\boldsymbol{x}^s, \boldsymbol{u}_1^s, \boldsymbol{u}_2^s + \boldsymbol{\delta}_{u_2}, \boldsymbol{\phi}\right) = \boldsymbol{0}$: Equality constraints for various operation states consists of power flow constrains and power balance constraints of VSCs.

For buses disconnected with VSCs, the power flow constrains can be written as

$$\begin{cases} P_{G,i}^{s_k} - P_{L,i}^{s_k} - U_i^{s_k} \sum\limits_{j \in N} U_j^{s_k}\left(g_{ij}^{s_k}\cos\theta_{ij}^{s_k} + b_{ij}^{s_k}\sin\theta_{ij}^{s_k}\right) = 0 \\ Q_{G,i}^{s_k} - Q_{L,i}^{s_k} - U_i^{s_k} \sum\limits_{j \in N} U_j^{s_k}\left(g_{ij}^{s_k}\sin\theta_{ij}^{s_k} - b_{ij}^{s_k}\cos\theta_{ij}^{s_k}\right) = 0 \end{cases} \tag{18}$$

with $\forall i \in N_A$ and $\forall s_k \in \Xi$.

For buses connected with VSCs, the power flow constraints can be written as

$$\begin{cases} P_{G,i}^{s_k} - P_{L,i}^{s_k} - \left(U_i^{s_k} + \delta_{U_i^{s_k}}\right) \sum\limits_{j \in N} U_j^{s_k}\left(g_{ij}^{s_k}\cos\theta_{ij}^{s_k}\right. \\ \left. +b_{ij}^{s_k}\sin\theta_{ij}^{s_k}\right) - \left(P_{S,i}^{s_k} + \delta_{P_{S,i}^{s_k}}\right) = 0 \\ Q_{G,i}^{s_k} - Q_{L,i}^{s_k} - \left(U_i^{s_k} + \delta_{U_i^{s_k}}\right) \sum\limits_{j \in N} U_j^{s_k}\left(g_{ij}^{s_k}\sin\theta_{ij}^{s_k}\right. \\ \left. -b_{ij}^{s_k}\cos\theta_{ij}^{s_k}\right) - \left(Q_{S,i}^{s_k} + \delta_{Q_{S,i}^{s_k}}\right) = 0 \end{cases} \tag{19}$$

with $\forall i \in N_D$ and $\forall s_k \in \Xi$. And based on (1) and (2), one gets

$$\begin{cases} P_{S,i}^{s_k} + \delta_{P_{S,i}^{s_k}} = -\left(U_i^{s_k} + \delta_{U_i^{s_k}}\right)^2 g_{tc,i} + \left(U_i^{s_k} + \delta_{U_i^{s_k}}\right) \\ \qquad \times U_{c,i}\left(g_{tc,i}\cos\alpha_i + b_{tc,i}\sin\alpha_i\right) \\ Q_{S,i}^{s_k} + \delta_{Q_{S,i}^{s_k}} = \left(U_i^{s_k} + \delta_{U_i^{s_k}}\right)^2 b_{tc,i} + \left(U_i^{s_k} + \delta_{U_i^{s_k}}\right) \\ \qquad \times U_{c,i}\left(g_{tc,i}\sin\alpha_i - b_{tc,i}\cos\alpha_i\right) \end{cases} \tag{20}$$

with $\forall i \in N_D$ and $\forall s_k \in \Xi$.

Based on (3), (5), (6), (7) and (8), power balance constraints of VSCs are given by (21) with $\forall (i,j) \in N_D{}'$, $\forall (j,i) \in N_D{}'$ and $\forall s_k \in \Xi$.

4) Constraints $\underline{\boldsymbol{g}}^s \leq \boldsymbol{g}^s\left(\boldsymbol{x}^s, \boldsymbol{u}_1^s, \boldsymbol{u}_2^s + \boldsymbol{\delta}_{u_2}, \boldsymbol{\phi}\right) \geq \overline{\boldsymbol{g}}^s$: For the AC grid, inequality constraints for various operation states mainly consists of voltage magnitude constraints, generator capability constraints and branch transmission capacity constraints as given by

$$\begin{cases} U_{i,\min}^{s_k} \leq U_i^{s_k} \leq U_{i,\max}^{s_k} & \forall i \in N_A, \forall s_k \in \Xi \\ U_{i,\min}^{s_k} \leq U_i^{s_k} + \delta_{U_i^{s_k}} \leq U_{i,\max}^{s_k} & \forall i \in N_D, \forall s_k \in \Xi \\ P_{G,i,\min} \leq P_{G,i}^{s_k} \leq P_{G,i,\max} & \forall i \in N_G, \forall s_k \in \Xi \\ Q_{G,i,\min} \leq Q_{G,i}^{s_k} \leq Q_{G,i,\max} & \forall i \in N_G, \forall s_k \in \Xi \\ S_{l,\min}^{s_k} \leq S_l^{s_k} \leq S_{l,\max}^{s_k} & \forall l \in L, \forall s_k \in \Xi \end{cases} \tag{22}$$

with $U_{i,\min}^{s_k}$, $P_{G,i,\min}$, $Q_{G,i,\min}$ and $S_{l,\min}^{s_k}$ denoting lower limits of corresponding variables, and $U_{i,\max}^{s_k}$, $P_{G,i,\max}$, $Q_{G,i,\max}$ and $S_{l,\max}^{s_k}$ denoting lower limits of corresponding variables.

And for the VSC-HVDC system, inequality constraints for various operation states consists of DC voltage constraints, voltage and current constraints of the AC side of converters and modulation index constraints as follows:

$$\begin{cases} U_{c,i,\min}^{s_k} \leq U_{c,i}^{s_k} \leq U_{c,i,\max}^{s_k} \\ \sqrt{\left(g_{tc,i}+b_{tc,i}\right)\left({U_{c,i}^{s_k}}^2+\left(U_{s,i}^{s_k}+\delta_{U_{s,i}}\right)^2-2U_{c,i}^{s_k}\left(U_{s,i}^{s_k}+\delta_{U_{s,i}}\right)\cos\alpha_i^{s_k}\right)} \\ \quad \leq I_{c,i,\max}^{s_k} \\ U_{dc,i,\min}^{s_k} \leq U_{dc,i}^{s_k} + \delta_{U_{dc,i}} \leq U_{dc,i,\max}^{s_k} \\ M_{i,\min} \leq \dfrac{\sqrt{2}U_{c,i}^{s_k}}{U_{dc,i}^{s_k} + \delta_{U_{dc,i}}} \leq M_{i,\max} \end{cases} \tag{23}$$

with $\forall i \in N_D$ and $\forall s_k \in \Xi$. And $U_{c,i,\min}^{s_k}$, $U_{dc,i,\min}^{s_k}$ and $M_{i,\min}$ denote the lower limits of corresponding variables, and $U_{c,i,\max}^{s_k}$, $I_{c,i,\max}^{s_k}$, $U_{dc,i,\max}^{s_k}$ and $M_{i,\max}$ denote the upper limits of corresponding variables.

5) Constraints $\boldsymbol{l}\left(\boldsymbol{x}^s, \boldsymbol{u}_1^s, \boldsymbol{u}_2^s + \boldsymbol{\delta}_{u_2}, \boldsymbol{\phi}\right) = \boldsymbol{0}$: Equality constraints coupling different operation states includes load power constraints, generator power constraints and control constraints for VSC-HVDC.

Assume that power factor remains the same as initial values when load power increasing and remains unchanged for operation states after a $N-1$ contingency. Load constraints are given by

$$\begin{cases} P_{L,i}^{s_k} = P_{L0,i}^{s_k} + \lambda_i \Delta P_{L,i}^{s_1} & \forall i \in N_L, \forall s_k \in \Xi \\ Q_{L,i}^{s_k} = Q_{L0,i}^{s_k} + \lambda_i \dfrac{\Delta P_{L,i}^{s_1} Q_{L0,i}^{s_1}}{P_{L0,i}^{s_1}} & \forall i \in N_L, \forall s_k \in \Xi \\ \lambda_i = \lambda_j & \forall i,j \in N_L \cap S_I, i \neq j \end{cases} . \tag{24}$$

Here $P_{L0,i}^{s_k}$ and $Q_{L0,i}^{s_k}$ denote initial active load power and initial reactive load power of bus i in the normal operation state, respectively. And $\Delta \boldsymbol{P}_L^{s_1} = [\Delta P_{L,1}^{s_1}, \cdots, \Delta P_{L,1}^{s_i}, \cdots]^{\mathrm{T}}$ with $i \in N_L$ is the given increase direction of active load power. The auxiliary variable λ_i represents the increase factor of load power. Note that the last term of (24) should be omitted if the load power increase direction is arbitrary.

Considering the calculation result of TTCU can be effected by changes of load power in the source area and generator power in the sink area, the following constraints w.r.t. λ_i and generator power should be satisfied:

$$\begin{cases} \lambda_i = 0 & \forall i \in N_L \cap S_O \\ P_{G,i}^{s_k} - P_{G0,i}^{s_1} = 0 & \forall i \in N_G \cap S_I, \forall s_k \in \Xi \\ Q_{G,i}^{s_k} - Q_{G0,i}^{s_1} = 0 & \forall i \in N_G \cap S_I, \forall s_k \in \Xi \end{cases} . \tag{25}$$

Here $P_{G0,i}^{s_1}$ and $Q_{G0,i}^{s_1}$ are initial generator active power and reactive power of bus i in the normal operation state, respectively.

Control constraints for VSC-HVDC are derived from the fact that control modes and fixed values of corresponding control parameters of converters remain unchanged after a $N-1$ contingency. The auxiliary boolean variables $c_{(i,j)}^r$ with $r = 1, 2, 3, 4$ and $\forall (i,j) \in N_D{}'$ are used to express the control modes of any VSC-HVDC system, i.e., $c_{(i,j)}^r = 1$ represents that the VSC-HVDC linnking terminal buses (i,j)

is controlled with the mode of combination r, and $c^r_{(i,j)} = 0$ represents that the VSC-HVDC linking terminal buses (i,j) is not controlled with the mode of combination r. And then control constraints for VSC-HVDC can be written as

$$\boldsymbol{C}\begin{bmatrix} \Delta\boldsymbol{U}_{dc,i} & \Delta\boldsymbol{Q}_{s,i} & \Delta\boldsymbol{P}_{s,j} & \Delta\boldsymbol{Q}_{s,j} \\ \Delta\boldsymbol{U}_{dc,i} & \Delta\boldsymbol{Q}_{s,i} & \Delta\boldsymbol{P}_{s,j} & \Delta\boldsymbol{U}_{s,j} \\ \Delta\boldsymbol{P}_{s,i} & \Delta\boldsymbol{Q}_{s,i} & \Delta\boldsymbol{U}_{dc,j} & \Delta\boldsymbol{U}_{s,j} \\ \Delta\boldsymbol{P}_{s,i} & \Delta\boldsymbol{U}_{s,i} & \Delta\boldsymbol{U}_{dc,j} & \Delta\boldsymbol{U}_{s,j} \end{bmatrix} = \boldsymbol{0} \quad \forall (i,j) \in N'_D. \tag{26}$$

Here $\boldsymbol{C} = \mathrm{diag}(\boldsymbol{C}^1_{(i,j)}, \boldsymbol{C}^2_{(i,j)}, \boldsymbol{C}^3_{(i,j)}, \boldsymbol{C}^4_{(i,j)})$ with $\boldsymbol{C}^1_{(i,j)}$ denoting a $1\times(|\Xi|-1)$ matrix block with all its entries being $c^1_{i,j}$, and $\boldsymbol{C}^2_{(i,j)}$, $\boldsymbol{C}^3_{(i,j)}$ and $\boldsymbol{C}^4_{(i,j)}$ being analogous. The $(|\Xi|-1)\times 1$ matrix block $\Delta\boldsymbol{U}_{dc,i}$ is with entries being $(U^{s_1}_{dc,i} - U^{s_k}_{dc,i})^2$ with $\forall s_f \in \Xi$ and $s_f \neq s_1$, and $\Delta\boldsymbol{Q}_{s,i}$, $\Delta\boldsymbol{P}_{s,i}$ and $\Delta\boldsymbol{U}_{s,i}$ are analogous. Besides, $c^r_{i,j}$ should satisfy the following constraint:

$$\sum_{r=1}^{4} c^r_{i,j} = 1 \quad \forall (i,j) \in {N_D}'. \tag{27}$$

For the given $c^r_{i,j}$, i.e., certain control combination of the VSC-HVDC linking terminal buses (i,j), control parameters corresponding to this control combination follow independent truncated normal distributions as described in Section II-B, and there is no uncertainties for control parameters of other control modes. For example, given $c^1_{i,j} = 1$ and $c^r_{i,j} = 0$ with $r \neq 1$, we have

$$\begin{cases} \delta_{U^{s_k}_{dc,i}} \sim \Pi(\mu_{U_{dc,i}}, \sigma_{U_{dc,i}}, \underline{t}_{U_{dc,i}}, \bar{t}_{U_{dc,i}}) \\ \delta_{Q^{s_k}_{s,i}} \sim \Pi(\mu_{Q_{s,i}}, \sigma_{Q_{s,i}}, \underline{t}_{Q_{s,i}}, \bar{t}_{Q_{s,i}}) \\ \delta_{U^{s_k}_{dc,j}} \sim \Pi(\mu_{U_{dc,j}}, \sigma_{U_{dc,j}}, \underline{t}_{U_{dc,j}}, \bar{t}_{U_{dc,j}}) \\ \delta_{U^{s_k}_{s,j}} \sim \Pi(\mu_{U_{s,j}}, \sigma_{U_{s,j}}, \underline{t}_{U_{s,j}}, \bar{t}_{U_{s,j}}) \\ \delta_{U^{s_k}_{s,i}} = \delta_{P^{s_k}_{s,i}} = \delta_{P^{s_k}_{s,j}} = \delta_{Q^{s_k}_{s,j}} = 0 \end{cases} \forall s_k \in \Xi. \tag{28}$$

And for other values of $c^r_{i,j}$, constraints of uncertainties of control parameters are analogous to (28).

C. The Solving Approach for the Calculation Model

The proposed calculation model for TTCU is a mixed-integer non-linear stochastic optimization model. In this paper, we do not focus on the efficient solving algorithm for the model. Simplistically, by firstly enumerating the integer variables and omitting the uncertainties, the optimization problem is decomposed into several non-linear sub-problems. Then given the solution of sub-problems, F' can be computed considering control parameter uncertainties, and finally the optimal solution of the original optimization model can be obtained by comparing the values of F' of all sub-problems.

IV. Case Study

The proposed calculation approach of TTCU is tested on the modified IEEE 39-bus system [9]. The diagram of this system is shown in Fig. 2 with adding a VSC-HVDC system between bus 13 and bus 16. And then the effects of control parameter uncertainties on TTC and the optimal operation of VSC-HVDC, and merits of TTCU are further discussed.

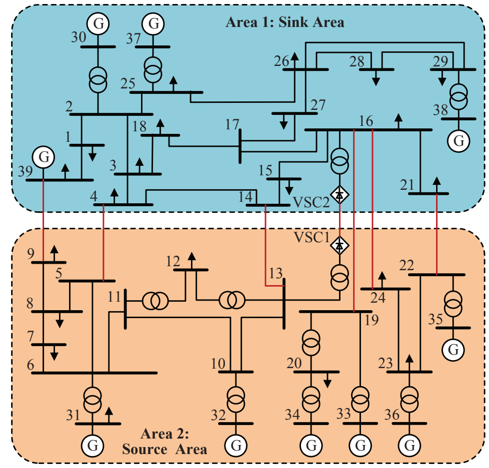

Fig. 2. Illustration of VSC-HVDC connected to the AC grid.

TABLE I
THE OPTIMAL CONTROL MODE AND VALUES OF CONTROL PARAMETERS CORRESPONDING TO TTCU

Converter	Optimal control mode	Optimal values of control parameters (p.u.)			
		$P_{s,i}$	$Q_{s,i}$	$U_{s,i}$	$U_{dc,i}$
VSC1	(3)	-	1.4705	-	0.9766
VSC2	(1)	-2.6816	0.7447	-	-

The non-linear optimization problems are solved using Pyomo with the solver IPOPT [10]. A 64-Bit computer with Intel(R) Core(TM) i7-6700 3.40GHz CPU, and 8GB RAM is used.

A. Parameter Settings

Considering that the original system operation state is critical and do not satisfy the $N-1$ security requirement, line 9-39 is replaced with a double-circuit line that each circuit is with the same parameters as the original single-circuit line, and load power of each load bus and generator power of each generator are all reduced by 50% to obtain the normal operation state. All $N-1$ contingencies of AC tie lines and branches in source area are considered.

As illustrated in Fig. 2, the area 1 and area 2 are sink area and source area respectively. And 7 tie lines, including 6 AC lines and 1 DC line connect these two areas. The load power increase direction of the sink area is assumed to be arbitrary.

For clarity, only the control parameter uncertainties of VSC1 are considered in our case study without loss of generality. And for the distribution of each control parameter uncertainty, we set $\mu = 0$, $\sigma = 0.02v$, $\underline{t} = 0.95v$ and $\bar{t} = 1.05v$ with v denoting the value of control parameters without uncertainties.

B. Calculation results of TTCU

By solving the TTCU calculation model consuming 3.43s computation time, the value of TTCU is 1932.59 MW, and the corresponding control model of converters and values of control parameters are given in TABLE I.

According to TABLE I, for reaching the TTC when considering the VSC1's control parameter uncertainties modeled

TABLE II
THE OPTIMAL CONTROL MODE AND VALUES OF CONTROL PARAMETERS CORRESPONDING TO TTC

Converter	Optimal control mode	Optimal values of control parameters (p.u.)			
		$P_{s,i}$	$Q_{s,i}$	$U_{s,i}$	$U_{dc,i}$
VSC1	(3)	-	1.5381	-	0.9781
VSC2	(2)	-2.7032	-	1.02312	-

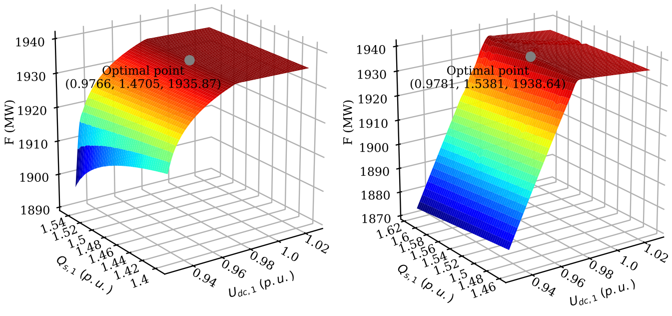

Fig. 3. $U_{dc,1}$-$Q_{s,1}$-F surface plots near the optimal point obtained under TTCU (left) and TTC (right). The bounds of $U_{dc,1}$ and $Q_{s,1}$ of the surface are both $\underline{t}$ and $\bar{t}$.

as the given independent truncated normal distributions, the VSC-HVDC system need to be operated in control mode of combination 1. And VSC1 is operated in control mode of constant $Q_{s,1}$ with 1.4705 p.u. and constant $U_{dc,1}$ with 0.9766 p.u., and VSC2 is operated in control mode of constant $P_{s,2}$ with -2.6816 p.u. and constant $Q_{s,2}$ with 0.7447 p.u..

C. Comparison with TTC and merits of TTCU

To demonstrate the effects of control parameter uncertainties on TTC and the optimal operation of VSC-HVDC, and also the merits of TTCU, the TTC of the system is computed using the calculation method in [7], as shortly described in Section I. The value of TTC is 1938.64 MW, and the corresponding optimal control mode and values of control parameters are given in TABLE II.

It can be found that TTCU is slightly lower than TTC, which means uncertainties of control parameters reduce TTC. Under the concept of TTCU, the actual values of control parameters are not equal to the optimal fixed values, but in its neighbourhood probabilistically. And more importantly, as shown in TABLE I and TABLE II, the optimal control mode of VSC2 and the optimal values of VSC1's control parameters corresponding to TTCU differ from that corresponding to TTC.

Fig. 3 gives the variation of transfer capability with control parameters of VSC1, i.e., $U_{dc,1}$ and $Q_{s,1}$, near the optimal point obtained under TTCU and TTC. Except for the control mode, other variables have all been optimized. It can be seen that the transfer capability is sensitive to control parameters of VSC1, especially $U_{dc,1}$, and thus the control parameter uncertainties in practice can greatly effects TTC. Although transfer capability in the optimal point obtained under TTC is larger than that in the optimal point obtained under TTCU, the $U_{dc,1}$-$Q_{s,1}$-F surface around the optimal point obtained under TTCU is with smaller overall curvature than that around the optimal point obtained under TTC. And thus when considering uncertainties of $U_{dc,1}$ and $Q_{s,1}$, the optimal point in the left plot of Fig. 3 becomes superior to that in the right plot w.r.t. transfer capability.

Compared with TTC, the merits of TTCU are twofold. First, TTCU embodies the reductions effect of control parameter uncertainties of VSC-HVDC to TTC and is more realistic, and the cost-benefit assessment of VSC-HVDC can be more accurate with TTCU. Second, the optimal control mode and fixed values of control parameters of VSC-HVDC obtained under TTCU can lead a more robust transfer capability. And this merit of TTCU is favourable for the optimal operation of the meshed girds with respect to transfer capability.

V. CONCLUSION

In this paper, a new concept called TTCU is proposed to address the issue of control parameter uncertainties in TTC calculation for meshed transmission grids with VSC-HVDC. And the calculation model of TTCU for meshed transmission grids with VSC-HVDC and its solving approach are further presented. By simulating on the modified IEEE 39-bus system, it is demonstrated that control parameter uncertainties of VSCs have a reductions effect on TTC and the optimal operation of VSC-HVDC with respect to TTC will be changed when considering these uncertainties. And compared with TTC, the proposed TTCU is more realistic by embodying the uncertainties' effect on TTC, and the optimal control mode and fixed values of control parameters of VSC-HVDC obtained under TTCU can lead a more robust transfer capability.

REFERENCES

[1] N. Flourentzou, V. G. Agelidis, and G. D. Demetriades, "Vsc-based hvdc power transmission systems: An overview," *IEEE Transactions on power electronics*, vol. 24, no. 3, pp. 592–602, 2009.

[2] J. Pan, R. Nuqui, K. Srivastava, T. Jonsson, P. Holmberg, and Y.-J. Hafner, "Ac grid with embedded vsc-hvdc for secure and efficient power delivery," in *Energy 2030 Conference, 2008. ENERGY 2008. IEEE*. IEEE, 2008, pp. 1–6.

[3] M. P. Bahrman and B. K. Johnson, "The abcs of hvdc transmission technologies," *IEEE power and energy magazine*, vol. 5, no. 2, pp. 32–44, 2007.

[4] T. T. C. T. Force, *Available transfer capability definitions and determination*. North American Electric Reliability Council, Princeton, New Jersey, 1996.

[5] G. Li and J. Zhang, "Available transfer capability calculation for ac/dc systems with vsc-hvdc," *Power System Protection and Control*, vol. 39, no. 1, pp. 46–52, 2011.

[6] G. Li and J. Zhang, "Available transfer capability calculation for ac/dc systems with vsc-hvdc," in *Electrical and Control Engineering (ICECE), 2010 International Conference on*. IEEE, 2010, pp. 3404–3409.

[7] T. Han, Y. Chen, Z. Han, K. Gao, S. Zhuan, and J. Ma, "Opf based total transfer capability calculation for ac-dc system with vsc-hvdc," *Automation of Electric Power Systems*, vol. 40, no. 17, pp. 113–121, 2016.

[8] C. P. Robert, "Simulation of truncated normal variables," *Statistics and computing*, vol. 5, no. 2, pp. 121–125, 1995.

[9] A. Pai, *Energy function analysis for power system stability*. Springer Science & Business Media, 2012.

[10] W. E. Hart, C. Laird, J.-P. Watson, and D. L. Woodruff, *Pyomo–optimization modeling in python*. Springer Science & Business Media, 2012, vol. 67.